博 士 論 文

Experience-dependent synaptic maintenance of layer 4–layer 2/3 synapse in the mouse barrel cortex

（マウス体性感覚野バレル皮質第 4 層―第 2/3 層シナプスにおける経験依存的シナプス機能維持）

久保田 淳

Experience-dependent synaptic maintenance of layer 4–layer 2/3 synapse in the mouse barrel cortex

マウス体性感覚野バレル皮質第 4 層―第 2/3 層シナプスにおける経験依存的シナプス機能維持

東京大学大学院医学系研究科　機能生物学専攻

細胞分子薬理学教室

久保田 淳

Contents

Summary

Sensory experience-dependent plasticity in the somatosensory cortex is a fundamental mechanism of adaptation to the changing environment not only early in the development but also in adolescence and adulthood. Although the mechanisms underlying experience-dependent plasticity during early development have been well documented, the corresponding understanding in the mature cortex is less complete. Here, I investigated the mechanism underlying whisker deprivation-induced synaptic plasticity in the barrel cortex in adolescent mice. Layer 4 (L4) to L2/3 excitatory synapses play a crucial role for whisker experience-dependent plasticity in rodent barrel cortex and whisker deprivation is known to depress synaptic strength at L4–L2/3 synapses in adolescent and adult animals. Whisker deprivation for 5 days or longer decreased the presynaptic glutamate release probability at L4–L2/3 synapses in the barrel cortex in adolescent mice. This whisker deprivation-induced depression was restored by daily administration of a positive allosteric modulator of the type 5 metabotropic glutamate receptor (mGluR5). On the other hand, the administration of mGluR5 antagonists reproduced the effect of whisker deprivation in whisker-intact mice. Furthermore, chronic and selective suppression of inositol 1,4,5-trisphosphate (IP_3) signaling in postsynaptic L2/3 pyramidal neurons decreased the presynaptic release probability at

L4–L2/3 synapses. These findings represent a previously unidentified mechanism of cortical plasticity, namely that whisker experience-dependent mGluR5-IP_3 signaling in the postsynaptic neurons maintains presynaptic function in the adolescent barrel cortex.

Introduction

A fundamental property of the brain is plasticity, ability to reorganize synaptic connections structurally and functionally, to adapt to changes in the internal and external state of individuals. The neocortex is particularly relevant for plasticity because it deals with dynamic changes in the information flow upon sensation, perception, cognition and action. One of the major cortical plasticity is the experience-dependent plasticity, which is the reorganization of cortical presentation of the sensory inputs upon sustained changes in the pattern of inputs (Feldman, 2009; Fox and Wong, 2005). While this experience-dependent plasticity is most robust during early development (Simons and Land, 1987; Vanderlo.H and Woolsey, 1973), adolescent and adult animals also display significant plasticity (Buonomano and Merzenich, 1998). We have a good understanding of the mechanisms underlying experience-dependent plasticity during early development, but our grasp of events in the mature cortex is less complete.

Rodent whiskers and their corresponding barrel cortex have been providing a ground for the study of experience-dependent plasticity. The barrels are cytoarchitectonic units in layer 4 (L4) of the somatosensory cortex that forms a topographic map corresponding to individual facial whiskers (Woolsey and Vanderlo.H, 1970). Excitatory L4 neurons make a

dense, monosynaptic feed-forward projection to L2/3 neurons within the same barrel column (Armstrongjames et al., 1992; Feldmeyer et al., 2002; Shepherd et al., 2003). Synaptic potentiation and depression at the ascending projection from L4 to L2/3 play a critical role in whisker experience-dependent plasticity (Feldman, 2009; Fox and Wong, 2005). Deprivation of whiskers in adolescent rats for 7 days weakens the responsiveness in L2/3 but not in L4 in the corresponding barrel cortex, strongly suggesting the depression of the L4–L2/3 synapses (Diamond et al., 1994; Fox, 2002; Glazewski and Fox, 1996; Stern et al., 2001). The mechanism responsible for deprivation-induced depression has been well characterized in younger animals. The reduction of the presynaptic release probability (P_r) at the L4–L2/3 synapse was induced upon the whisker deprivation for at least 3 days starting from postnatal day 12 (P12) to P19 in rats (Bender et al., 2006a; Li et al., 2009). This P_r reduction has been implicated in a spike-timing dependent plasticity involving *N*-methyl-D-aspartic acid receptor (NMDAR), group I metabotropic glutamate receptor (mGluR), and type 1 cannabinoid receptor (CB1R) (Allen et al., 2003; Bender et al., 2006b; Celikel et al., 2004; Li et al., 2009; Min and Nevian, 2012; Rodriguez-Moreno and Paulsen, 2008). Actually, pharmacological inhibition of CB1R disrupts the whisker map precision and whisker deprivation-induced depression in the barrel cortex of rats up to P25 (Li et al., 2009). However, the mechanism for whisker deprivation-induced synaptic depression in older animals is poorly understood. A

previous study has shown that whisker deprivation starting from P33 induces cortical synaptic depression independently of CB1R in rats (Li et al., 2009), indicating a developmental change in the mechanism.

Here I investigated the mechanism underlying CB1R-independent plasticity induced by whisker deprivation in adolescent mice. The results indicate that ongoing whisker input-dependent activation of mGluR5 is required for the maintenance of presynaptic function at the L4–L2/3 synapses. In addition, the suppression of inositol 1,4,5-trisphosphate (IP_3) production in L2/3 pyramidal neurons decreased P_r at L4–L2/3 synapses. These findings indicate that whisker experience-dependent mGluR5-IP_3 signaling in postsynaptic L2/3 neurons maintains P_r and that shutdown of this signaling pathway by whisker deprivation results in presynaptic attenuation in the barrel cortex of adolescent mice. This is a previously unrecognized mechanism that sheds new light on cortical plasticity.

This thesis is written on the basis of my recently published paper (Kubota et al., 2016).

Materials and methods

Whisker deprivation and drug administration

All animal experiments were performed in accordance with the regulations and guidelines for Institutional Animal Care and Use Committee at The University of Tokyo and were approved by the institutional review committees of Graduate School of Medicine, The University of Tokyo. For whisker deprivation, all large whiskers of C57/B6N mice (Nihon SLC, Shizuoka, Japan) of either sex were plucked from the left side under isoflurane anesthesia (~2% in O_2, vol/vol; Mylan, Canonsburg, PA, USA). The left mystacial pad was coated with lidocaine gel (AstraZeneca, London, UK) to provide local analgesia. Sham-operated littermates were anesthetized and handled identically, but whiskers were not plucked. Whisker-deprivation was maintained by plucking every other day until slices were prepared. *N*-(Piperidin-1-yl)-5-(4-iodophenyl)-1-(2,4-dichlorophenyl)-4-methyl-1*H*-pyrazole-3-carboxamide (AM251), 2-methyl-6-(phenylethynyl)pyridine hydrochloride (MPEP), and (*RS*)-1-aminoindan-1,5-dicarboxylic acid (AIDA) were dissolved in vehicle solution (0.9% NaCl). 3-Cyano-N-(1,3-diphenyl-1H-pyrazol-5-yl)benzamide (CDPPB) was suspended in a vehicle containing 20% (2-hydroxypropyl)-(R)-cyclodextrin (Sigma-Aldrich, St. Louis, MO,

USA) in sterile saline. The drugs were applied by intraperitoneal (i.p.) injection, and were obtained from Tocris Cookson (Ellisville, MO, USA).

Slice preparation

Slices were prepared by two different ways according to the age of the animal. Younger mice (<P25) were handled as described previously (Edwards et al., 1989). In brief, coronal slices of the barrel cortex of 300 µm thickness were cut using a microslicer (PRO7; Dosaka EM, Kyoto, Japan) in ice-cold cutting solution containing (in mM) 110 choline chloride, 2.5 KCl, 1.25 NaH_2PO_4, 25 $NaHCO_3$, 25 D(+)-glucose, 3.1 sodium pyruvate, 11.6 sodium ascorbate, 0.5 $CaCl_2$ and 7 $MgCl_2$ (oxygenated by 95% O_2 and 5% CO_2). Slices were incubated in oxygenated normal artificial cerebrospinal fluid [ACSF: 125 NaCl, 2.5 KCl, 1.25 NaH_2PO_4, 26 $NaHCO_3$, 25 D(+)-Glucose, 2 $CaCl_2$ and 1 $MgCl_2$] at 32°C for 30 min and then stored at room temperature (RT, 21–25°C).

Older mice (>P40) were anesthetized with intraperitoneal injection of ketamine and medetomidine (75 mg kg^{-1} and 1 mg kg^{-1}, respectively) or medetomidine, midazolam and butorphanol (0.75 mg kg^{-1}, 4 mg kg^{-1} and 5 mg kg^{-1}, respectively) and transcardially perfused with ice-cold oxygenated protective ACSF: 92 N-methyl-D-glucamine (NMDG), 2.5 KCl, 1.25 NaH_2PO_4, 30 $NaHCO_3$, 20 HEPES, 25 D(+)-Glucose, 2 thiourea, 5 sodium

ascorbate, 3 sodium pyruvate, 0.5 $CaCl_2$ and 10 $MgSO_4$ (pH 7.3–7.4, adjusted with HCl). Mice were then decapitated and brains were removed into ice-cold oxygenated protective ACSF. Brains were then rapidly embedded in 1.5% low-melting-point agarose (Sigma-Aldrich or Lonza, Basel, Switzerland) and coronal slices of 300 µm thickness were cut using VF300 Compresstome (Precisionary Instruments, Greenville, NC, USA). Some slices were also cut using a microslicer in ice-cold oxygenated protective ACSF. Slices were allowed to recover for 10–15 min at 32–34°C in oxygenated protective ACSF then transferred into oxygenated holding ACSF at RT (Zhao et al., 2011). The holding ACSF was similar to the protective ACSF except that NMDG was replaced by equimolar NaCl.

Electrophysiology

Slices were placed in a recording chamber that was continuously superfused with oxygenated ACSF. All recordings were performed at RT. Barrels were visualized under bright field illumination. L2/3 pyramidal neurons were visualized using an upright infrared-differential interference contrast microscope (BX61WI; Olympus, Tokyo, Japan) equipped with a water-immersion objective (60×, numerical aperture = 0.90; Olympus). Whole-cell patch clamp recordings were performed with 4–8 MΩ pipettes using an EPC-9 patch clamp amplifier (HEKA, Electronik, Lambrecht/Pfalz, Germany). For voltage-clamp recordings, the

internal solution contained the following (in mM): 100 D(+)-gluconic acid, 100 CsOH, 20 CsCl, 10 Cs-HEPES, 4 MgATP, 0.3 Na_3GTP, 10 Na_2-phosphocreatine (pH 7.2–7.4, 290–300 mOsm, adjusted with CsOH and sucrose). For current-clamp recordings, the internal solution contained the following (in mM): 100 K gluconate, 20 KCl, 10 K-HEPES, 4 MgATP, 0.3 Na_3GTP, 10 Na_2-phosphocreatine (pH 7.2–7.4, 290–300 mOsm, adjusted with KOH and sucrose). Series resistance (10–50 MΩ) was not statistically different between experimental groups (e.g. Sham, 28.1 ± 5.0 MΩ; Deprived for 3 days, 29.7 ± 5.9 MΩ; Deprived for 5–7 days, 27.5 ± 5.6 MΩ for Figure 1C, $5ppase^{Intact}$, 24.4 ± 5.0 MΩ; $5ppase^{WT}$, 25.7 ± 4.8MΩ for Figure 9B) and not compensated. Alexa Fluor 594 (50 μM; Invitrogen, Carlsbad, CA, USA) was added to the internal solution and pyramidal neuron morphologies were confirmed by custom-made two-photon microscopy (Okubo et al., 2004; Okubo et al., 2010). A glass pipette with a 5–10 μm tip diameter filled with normal ACSF was placed in the geometric center of an L4 barrel below the patched L2/3 pyramidal neuron (See also Figure 1B). The intensities of the square pulses for the focal stimulation (0.9–9.0 V, 0.1 ms) were adjusted to induce excitatory postsynaptic currents (EPSCs) with amplitudes of approximately 200 pA to provide stable and reproducible recordings. Data were filtered at 3 kHz and digitized at 20 kHz. Online data acquisition and offline analysis were performed using the PULSE and PULSE-FIT programs (HEKA), respectively.

For paired-pulse ratio (PPR) measurements, α-amino-3-hydroxy-5-methyl-4-isoxazolepropionic acid receptor (AMPAR)-mediated currents were isolated in the presence of the NMDAR antagonist, D-(-)-2-amino-5-phosphonopentanoic acid (D-AP5, 50 μM), and measured at −70 mV holding potential. PPR was defined as the ratio of the amplitudes of two sequential EPSCs evoked with a 50-ms interval. When the second pulse overlapped with the decay of the first, the tail of the first EPSC was subtracted from the second. For P_r measurement using 11-dihydro-5H-dibenzo[a,d]cyclohepten-5,10-imine maleate (MK-801), NMDAR-mediated currents were isolated in the presence of the AMPAR antagonist 2,3-dioxo-6-nitro-1,2,3,4-tetrahydrobenzo[f]quinoxaline-7-sulfonamide (10 μM) and measured at +40 mV holding potential. In the presence of MK-801 (10 μM), stimulation was applied every 15 s to induce progressive decay of EPSC amplitude. EPSC amplitude was normalized for each cell to the first EPSC. Decay time courses were fitted to a double exponential function using Igor Pro (WaveMetrics, Portland, OR, USA), and the time constant of the fast component was used for the evaluation of P_r. For quantal EPSC measurements, AMPAR-mediated EPSCs were isolated with D-AP5 (50 μM) and measured at −70 mV holding potential. By replacing $CaCl_2$ with 3 mM $SrCl_2$, asynchronous vesicle release was induced. Quantal EPSCs occurring

200–500 ms after stimulus onset were analyzed. The frequency of quantal EPSCs was 23–30 Hz throughout the experiments.

Construction and infection of adeno-associated viruses

The wild-type IP_3 5-phosphatase ($5ppase^{WT}$) and the catalytically inactive mutant (R343A/R350A) $5ppase^{Inact}$ were described previously (Kanemaru et al., 2007). A hemagglutinin (HA) tag was added to the N terminus of each 5ppase. The picornaviral (porcine teschovirus-1) 2A (P2A) peptide-linked multicistronic construct, tdTomato-P2A-HA-$5ppase^{WT}$ or $5ppase^{Inact}$, was generated as described previously (Holst et al., 2006). A fluorescent protein, tdTomato, was used as an infection marker. The adeno-associated virus (AAV) construct pAAV-CaMKIIα-tdTomato-P2A-HA-$5ppase^{WT}$ or $5ppase^{Inact}$ was made by subcloning into pAAV-CaMKIIα-EGFP (Addgene #50469). The pXR9 plasmid (AAV9; National Gene Vector Biorepository, IN, USA) and the pHelper plasmid were co-transfected into HEK293T cells with polyethylenimine (Polyethylenimine "Max," Polysciences, Warrington, PA, USA). After 72 h of incubation, culture media and cell lysates were collected, subjected to three-times of freeze-thaw cycles, and then centrifuged in a CsCl gradient to obtain a suspension containing AAV9-CaMKIIα-tdTomato-P2A-HA-$5ppase^{WT}$ or $5ppase^{Inact}$. In some cases, an AAV

extraction solution (AAVpro Extraction Solution, Takara Bio Inc., Shiga, Japan) was applied instead of using the above-described procedure. Viruses were concentrated using centrifugal filter units (Amicon Ultra-15, 50 kDa normal molecular weight limit; Millipore, Bedford, MA, USA), and suspended with HN buffer (50 mM HEPES and 150 mM NaCl; pH adjusted to 7.4 with NaOH). Virus titers were determined by measuring the number of encapsidated genomes with quantitative real-time polymerase chain reaction analysis (Power SYBR Green PCR Master Mix; Applied Biosystems, Foster City, CA, USA). The AAV9-CaMKIIα-tdTomato-P2A-HA-5ppase^{WT} was obtained at a concentration of 0.7–8.0 × 10^{12} genome copies per mL (gc mL^{-1}), and AAV9-CaMKIIα-tdTomato-P2A-HA-5ppase^{Inact} was obtained at 1.3–7.0 × 10^{12} gc mL^{-1}.

Mice (P28–32) were anesthetized with an intraperitoneal injection of medetomidine, midazolam, and butorphanol (0.75 mg kg^{-1}, 4 mg kg^{-1}, and 5 mg kg^{-1}, respectively). The anesthesia was maintained with isoflurane (typically 1% mixed with O_2) as needed. The skull was exposed, and small craniotomies (diameter, <500 μm) were performed at 1.0–1.1 mm posterior and 3.0–3.2 mm lateral from the bregma. Then, 100–200 nL of either AAV9-CaMKIIα-tdTomato-P2A-HA-5ppase^{WT} or 5ppase^{Inact} was delivered into the barrel cortex, targeting L2/3 (approximately 300 μm below the pial surface), using a glass pipette (outer diameter of 20–30 μm, beveled at an angle of 30°) and a micropump (KDS-310;

Muromachi Kikai, Tokyo, Japan) at a rate of 20 nL min^{-1}. The pipette was left in place for more than 20 min to prevent leakage of the solution. At 14–18 days after the virus injection, slices were prepared as described above. Infected cells were identified by the tdTomato fluorescence. Patch clamp recording was performed on the infected L2/3 pyramidal cells in the column in which infected cells were preferentially observed within L2/3. Samples with a significant spread of infected cells into L4 and deeper layers were discarded.

Primary culture and Ca^{2+} imaging

Primary cultures of cortical neurons were prepared as described previously (Kakizawa et al., 2012; Kanemaru et al., 2007). Briefly, minced cerebral cortices from embryonic mice (embryonic day 16) were treated with 1.0% (w/v) trypsin (Wako) and 0.1% (w/v) deoxyribonuclease I (Sigma-Aldrich) in Ca^{2+}/Mg^{2+}-free phosphate-buffered saline (PBS) for 5 min at RT. Cells were washed with Neurobasal-A medium (Gibco, ThermoFisher Scientific, Grand Island, NY, USA) supplemented with 5% (v/v) fetal bovine serum (FBS; Gibco), penicillin (100 units mL^{-1}; Gibco), streptomycin (100 units mL^{-1}; Gibco), B-27 supplement (Gibco), and 2 mM L-glutamine (Gibco) and dissociated by triturating with a fire-polished Pasteur pipette in Ca^{2+}/Mg^{2+}-free PBS containing 0.05% (w/v) deoxyribonuclease I and 0.03% (w/v) trypsin inhibitor (Sigma-Aldrich). The cell suspension was poured through a

40-μm cell strainer. Dispersed cells were plated at 1.0×10^5 cells cm^{-2} on glass slides coated with poly-L-lysine and laminin (Sigma-Aldrich). Cells were then cultured at 37°C under a humidified atmosphere containing 5% CO_2. The medium was changed every 2 days by replacing half of the old medium with fresh FBS-free medium. Primary cultured neurons at 4 days *in vitro* were infected with AAV9-CaMKIIα-tdTomato-P2A-HA-5ppase^{WT} or 5ppase^{Inact}. Ten days after infection, neurons were examined for Ca^{2+} imaging.

The Ca^{2+} imaging was conducted as described previously (Kakizawa et al., 2012). Briefly, neurons were loaded with 5 μM Fura-2 AM (Molecular Probes, ThermoFisher Scientific, Eugene, OR, USA) for 30 min in HEPES-buffered saline (150 mM NaCl, 4 mM KCI, 2 mM $CaCl_2$, 1 mM $MgCl_2$, 5 mM HEPES, 5.6 mM glucose, pH adjusted to 7.4 with NaOH). Fluorescence images were acquired using an inverted microscope (IX81, Olympus) with a UApo/340 40× (numerical aperture, 1.35; Olympus) and a cooled CCD camera (EM-CCD C9100, Hamamatsu Photonics, Shizuoka, Japan) at a rate of one frame every 3 s. Excitation wavelengths were 340 and 380 nm. Experiments were conducted at RT. The ratio of the fluorescence intensity at each excitation wavelength (F_{340}/F_{380}) was calculated using ImageJ64 (National Institutes of Health, Bethesda, MD, USA). Immediately before Ca^{2+} imaging, tetrodotoxin (1 μM) was applied to block action potentials. At the end of the experiments, the responsiveness of the imaged neurons was confirmed by examining

glutamate (100 μM)-induced Ca^{2+} responses (0.36 ± 0.02 for $5ppase^{WT}$, 0.39 ± 0.02 for $5ppase^{Inact}$; mean ± SEM).

Statistical analysis

All values are expressed as mean ± SEM. Statistical analyses were performed using Microsoft Excel and R version 3.1.2 (The R Foundation for Statistical Computing). The two-tailed Student *t*-test was applied on single comparisons between two groups. One-way analysis of variance (ANOVA) with Tukey's honestly significant difference (HSD) *post hoc* test was used when comparing data from three groups. The Kolmogorov–Smirnov test was used to compare the cumulative probability distributions of quantal EPSC. The asterisks in the figures indicate the following: $*P < 0.05$, $**P < 0.01$, and $***P < 0.001$.

Results

CB1R-independent presynaptic depression following whisker deprivation in mice after P18

To study the mechanism underlying CB1R-independent depression induced by whisker deprivation in adolescent rodents, I examined the effect of whisker deprivation at P18–20 on L4–L2/3 synapses in mice. All large whiskers were plucked unilaterally to circumvent possible heterosynaptic effects induced by non-deprived neighboring whiskers (Allen et al., 2003; Feldman and Brecht, 2005; Glazewski et al., 1998; Stern et al., 2001; Wallace and Fox, 1999). Whisker deprivation was continued for either 3 or 5–7 days before slice preparations of the barrel cortex and electrophysiological evaluation of L4–L2/3 synapses (Figures 1A and 1B).

Previous studies have shown that whisker deprivation in younger rats induces an increase in PPR at L4–L2/3 synapses (Bender et al., 2006a; Li et al., 2009). PPR is defined as the ratio of two sequential postsynaptic currents or potentials, and is considered to be inversely related to P_r at glutamatergic terminals (Zucker and Regehr, 2002). Although postsynaptic AMPAR desensitization upon repetitive inputs is also involved in the changes in PPR at certain synapses (Otis et al., 1996), this is not the case at L4–L2/3 synapses (Bender et

al., 2006a). These previous results prompted me to measure PPR by recording EPSCs from L2/3 pyramidal neurons following a pair of L4 stimulations separated by 50 ms (Figure 1C). Three days of deprivation did not induce significant changes in PPR, but 5–7 days of deprivation significantly increased PPR [Sham for 5–7 days, 0.79 ± 0.03, n = 7 cells (6 mice); Deprived for 3 days, 0.81 ± 0.03, n = 6 cells (5 mice); Deprived for 5–7 days, 0.95 ± 0.04, n = 7 cells (7 mice); $F_{2,17}$ = 8.77, P = 0.003 Sham for 5–7 days vs. Deprived for 5–7 days, P = 0.01 Deprived for 3 days vs. Deprived for 5–7 days, one-way ANOVA with Tukey's HSD *post hoc* test; Figure 1C]. To evaluate the potential effect of inhibitory postsynaptic currents (IPSCs) on PPR measurements, I also performed PPR recordings at −50 mV, which is near the reversal potential of IPSCs. I found slight increases in PPR at −50 mV compared with those observed at −70 mV. Similar slight increases were observed in both whisker-deprived and non-deprived mice (PPR at −70 mV vs. PPR at −50 mV: 0.95 ± 0.04 vs. 1.08 ± 0.03 in whisker-deprived mice; 0.79 ± 0.03 vs. 0.90 ± 0.04 in non-deprived mice; mean ± SEM). Therefore, the potential effect of IPSCs, if any, should not affect the conclusion obtained by recordings at −70 mV. This strongly suggests that whisker deprivation after P18 reduces P_r at L4–L2/3 synapses.

I further confirmed the decrease in P_r using MK-801, an irreversible open-channel blocker of NMDAR. NMDAR-mediated EPSCs are use-dependently blocked in the presence

of MK-801, and the time constant of this blockade is inversely related to P_r (Hessler et al., 1993; Rosenmund et al., 1993). MK-801 blockade was slower in whisker-deprived mice [Sham, 5.44 ± 1.02 stimuli, n = 4 cells (4 mice); Deprived, 16.62 ± 0.91 stimuli, n = 5 cells (5 mice); $t_7 = -8.17$, $P = 0.00008$, two-tailed unpaired Student's t-test; Figure 2A and 2B], confirming P_r reduction at L4–L2/3 synapses.

I next determined if postsynaptic glutamate responsiveness was altered by whisker deprivation. Quantal size variations of asynchronous EPSCs in the presence of Sr^{2+} (Goda and Stevens, 1994; Oliet et al., 1996) at L4–L2/3 synapses were distributed identically in deprived and sham-deprived mice [Sham, 336 events from 7 cells (6 mice); Deprived, 345 events from 7 cells (7 mice); P = 0.30, Kolmogorov–Smirnov test; Figure 2C], indicating that whisker deprivation after P18 induces presynaptic depression at L4–L2/3 synapses without affecting the postsynaptic responsiveness.

I investigated whether the deprivation-induced plasticity observed above is mediated by a mechanism distinct from that previously reported in younger animals. Previous studies reported a CB1R-dependent increase in PPR at L4–L2/3 synapses following one-row whisker deprivation beginning at P16–19 in rats (Bender et al., 2006a; Bender et al., 2006b; Li et al., 2009). Therefore, I first confirmed whether my experimental procedure, that is, all whisker deprivation in mice, could reproduce the CB1R-dependent mechanism in younger mice.

Whisker deprivation performed same as above but starting from P12–14 increased PPR, and this PPR increase was completely blocked by daily administration of the CB1R antagonist AM251 [Sham, 0.70 ± 0.02, n = 6 (5 mice); Deprived, 1.06 ± 0.04, n = 6 (6 mice); Deprived + AM251, 0.73 ± 0.06, n = 5 (4 mice); $F_{2,14}$ = 26.75, P = 0.00003 Sham vs. Deprived, P = 0.0001 Deprived vs. Deprived + AM251, one-way ANOVA with Tukey's HSD *post hoc* test; Figures 3A and 3B]. On the other hand, when whisker deprivation was performed beginning at P18–20, the administration of AM251 had very little effect on the PPR increase, indicating the involvement of a CB1R-independent mechanism [Sham, 0.79 ± 0.03, n = 7 cells (6 mice); Deprived, 0.95 ± 0.04, n = 7 cells (7 mice); Deprived + AM251, 0.88 ± 0.03, n = 6 (6 mice); $F_{(2,17)}$ = 8.11, P = 0.002 Sham vs. Deprived, P = 0.28 Deprived vs. Deprived + AM251, one-way ANOVA with Tukey's HSD *post hoc* test; Figures 3A and 3B]. These results do not rule out the possibility that a modest contribution of CB1R-dependent mechanism remains in mice after P18. In fact, a CB1R-dependent P_r reduction has been reported in the barrel cortex of rats as old as P23 (Bender et al., 2006b). In conclusion, the presynaptic depression induced by all whisker deprivation in mice at P18–20 is mainly mediated by a synaptic mechanism distinct from that in younger animals.

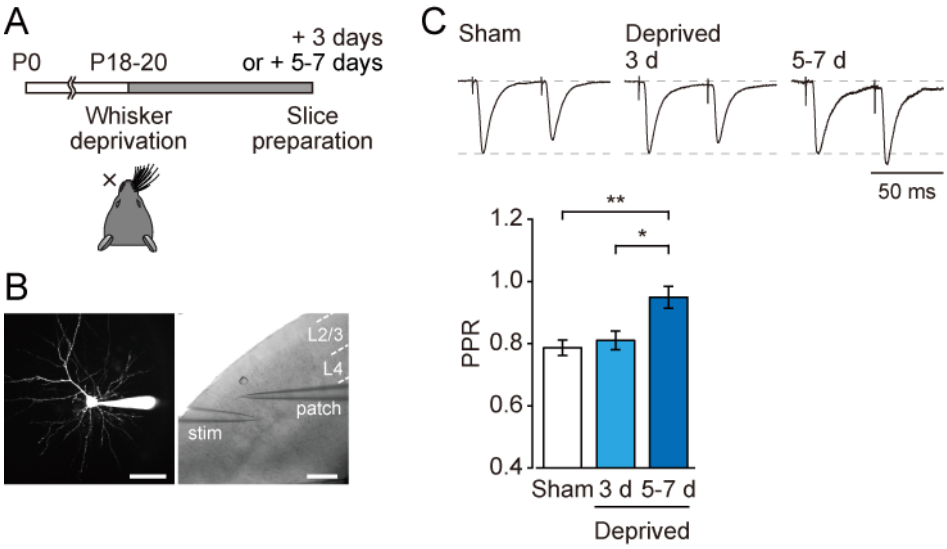

Figure 1. Whisker deprivation after P18 increases PPR at L4–L2/3 synapses.
(A) Schema of experimental procedure. At P18–20, all large whiskers were plucked from the left side. Whisker deprivation was continued for either 3 or 5–7 days before slice preparation. (B) Whole-cell voltage-clamp recordings were performed in L2/3 pyramidal neurons. Morphology was maximum intensity projection of Alexa 594 fluorescence obtained with two-photon laser scanning microscopy, verifying that patched cells were pyramidal neurons. And focal stimulations were applied through a glass pipette placed on the center of L4 barrel. Scale bar, 50 μm and 500 μm, respectively.
(C) (*Upper*) Representative recordings of PPR. (*Lower*) Summary graph of PPR. At least 5 days of whisker-deprivation is required to increase PPR. Mean ± SEM [n = 7 (6 mice) for Sham (5–7 days), n = 6 (5 mice) for Deprived (3 days) and n = 7 (7 mice) for Deprived (5–7 days)]. *P < 0.05, **P < 0.01, one-way ANOVA with Tukey's HSD *post hoc* test.

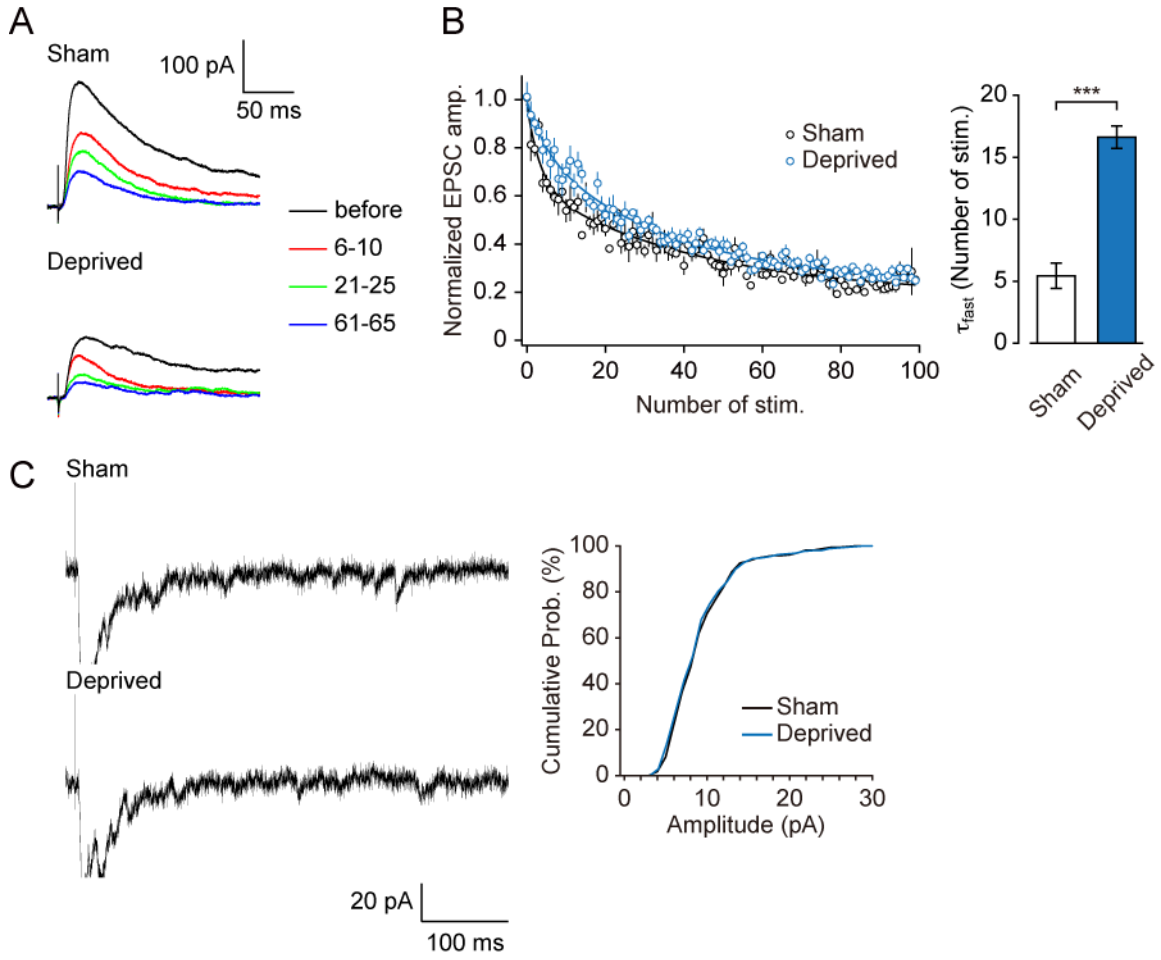

Figure 2. Whisker deprivation after P18 reduces P_r at L4–L2/3 synapses.

(A, B) Measurement of P_r using MK-801. (A) Representative traces of NMDAR-EPSCs before and after the application of MK-801 (average of 5 sweeps). Key indicates corresponding stimulus sequence numbers. (B) (*Left*) Decay of NMDAR-mediated EPSC in the presence of MK-801 (10 μM). (*Right*) Summary of decay time constant of EPSC amplitude. Mean ± SEM [n = 4 (4 mice) for Sham, n = 5 (5 mice) for Deprived]. ***P < 0.001, two-tailed unpaired Student's t-test.

(C) (*Left*) Representative recordings of quantal EPSCs in ACSF containing Sr^{2+} (3 mM). (*Right*) Cumulative histogram showing the distribution of quantal EPSC amplitude. p = 0.298, Kolmogorov–Smirnov test [Sham; 336 events from 7 cells (6 mice), Deprived; 345 events from 7 cells (7 mice)].

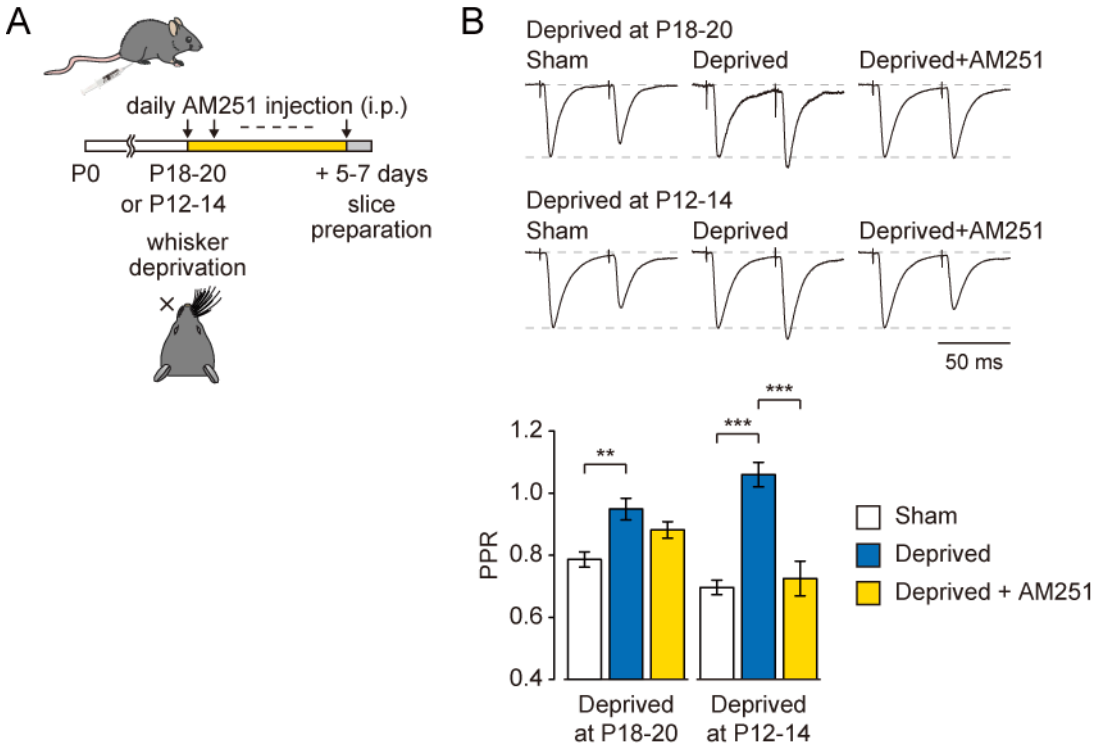

Figure 3. CB1R-independent depression at L4–L2/3 synapses upon whisker deprivation after P18.

(A) Schema of experiment procedure. Whisker deprivation was performed at either P18–20 or P12–14 and the animals were given daily administration of AM251 (10 mg kg^{-1}, i.p.) for 5–7 days before slice preparation.

(B) (*Upper*) Representative recordings of PPR. (*Lower*) Summary of AM251 effects on PPR. AM251 blocked PPR increase upon whisker deprivation at P12–14 but not at P18–20. Sham and Deprived in P18–20 are the same data as in (Figure. 1C). Mean ± SEM [n = 7 (6 mice) for Sham, n = 7 (7 mice) for Deprived and n = 6 (6 mice) for Deprived + AM251 in P18–20, n = 6 (5 mice) for Sham, n = 6 (6 mice) for Deprived and n = 5 (4 mice) for Deprived + AM251 in P12–14]. $^{**}P < 0.01$, $^{***}P < 0.001$, one-way ANOVA with Tukey's HSD *post hoc* test.

Whisker input-evoked mGluR5 signaling maintains P_r in adolescent mice

I next assessed signaling mechanisms that might mediate the CB1R-independent presynaptic depression in adolescent mice. Previously, our laboratory reported an mGluR-dependent P_r maintenance mechanism at the parallel fiber-Purkinje cell synapses in the cerebellum (Furutani et al., 2006). I hypothesized that a similar mGluR-dependent mechanism is involved in the maintenance of L4–L2/3 synapses, and that whisker deprivation suppresses the ongoing P_r maintenance mechanism. To test this, I performed daily administration of CDPPB, a positive allosteric modulator of mGluR5, to potentiate the mGluR5 activity in mice whose whiskers were deprived at P18–20. CDPPB reversed the whisker deprivation-induced PPR increase [Sham, 0.79 ± 0.03, n = 7 cells (6 mice); Deprived, 0.95 ± 0.04, n = 7 cells (7 mice); Deprived + CDPPB, 0.72 ± 0.06, n = 6 (4 mice); $F_{2,17}$ = 8.85, P = 0.03 Sham vs. Deprived, P = 0.002 Deprived vs. Deprived + CDPPB, one-way ANOVA with Tukey's HSD *post hoc* test; Figures 4A and 4B], suggesting that mGluR5 is involved in the P_r maintenance in adolescent mice. I then examined the involvement of this mGluR5-dependent mechanism in younger mice. Daily administration of CDPPB in mice whose whiskers were plucked at P12–14 failed to reverse the whisker deprivation-induced PPR increase [Sham, 0.70 ± 0.02, n = 6 cells (5 mice); Deprived, 1.06 ± 0.04, n = 6 cells (6 mice); Deprived + CDPPB, 1.08 ± 0.06, n = 6 cells (4 mice); $F_{2,15}$ = 23.86, P = 0.0001

Sham vs. Deprived, P = 0.00005 Deprived vs. Deprived + CDPPB, one-way ANOVA with Tukey's HSD *post hoc* test; Figures 4A and 4B]. To further confirm mGluR5-dependent P_r maintenance mechanism, I tested whether pharmacological blockade of mGluR5 reproduced the effect of whisker deprivation on L4–L2/3 synapses in whisker-intact mice. Administration of AIDA (a selective antagonist of group I mGluR) or MPEP (an mGluR5-selective antagonist) to whisker-intact mice significantly increased PPR [Vehicle, 0.77 ± 0.02, n = 7 cells (7 mice); AIDA, 1.04 ± 0.06, n = 6 cells (6 mice); MPEP, 0.94 ± 0.05, n = 6 cells (6 mice); $F_{2,16}$ = 9.12, P = 0.0019 Vehicle vs. AIDA, P = 0.046 Vehicle vs. MPEP, one-way ANOVA with Tukey's HSD *post hoc* test Figure 5A]. AIDA and MPEP-induced reduction of P_r was confirmed by the MK-801 assay [Vehicle, 4.32 ± 0.94 stimuli, n = 4 cells (4 mice); AIDA, 15.53 ± 0.71 stimuli, n = 4 cells (4 mice); MPEP, 15.45 ± 0.74 stimuli, n = 4 cells (4 mice); $F_{2,9}$ = 64.88, P = 0.00001 Vehicle vs. AIDA, P = 0.00001 Vehicle vs. MPEP, one-way ANOVA with Tukey's HSD *post hoc* test; Figures 5B and 5C] while the absence of an effect of AIDA and MPEP on postsynaptic glutamate responsiveness was confirmed by Sr^{2+}-induced asynchronous EPSC responses [Vehicle, 313 events from 6 cells (6 mice); AIDA, 308 events from 6 cells (6 mice); MPEP, 311 events from 6 cells (6 mice); P = 0.30 AIDA vs. Vehicle, P = 0.99 MPEP vs. Vehicle, Kolmogorov–Smirnov test; Figure 5D]. Thus, administration of mGluR5 antagonists reproduced the effect of whisker deprivation. These

results indicate that ongoing whisker input-evoked mGluR5 signaling is essential for the maintenance of P_r in mice after P18. This previously unrecognized mechanism can account for experience deprivation-induced depression in the barrel cortex. I examined whether this mechanism regulates P_r in later stages of adolescence. Whisker deprivation after P33 resulted in an increase in PPR at L4–L2/3 synapses and the administration of CDPPB blocked this effect [Sham, 0.93 ± 0.05, n = 5 cells (5 mice); Deprived, 1.20 ± 0.05, n = 6 cells (5 mice); Deprived + CDPPB, 0.99 ± 0.04, n = 5 (5 mice); $F_{2,13}$ = 7.98, P = 0.006 Sham vs. Deprived, P = 0.03 Deprived vs. Deprived + CDPPB, one-way ANOVA with Tukey's HSD *post hoc* test; Figures 6A and 6B]. Administration of AIDA or MPEP to whisker-intact mice older than P39 also increased PPR, mimicking the effect of whisker deprivation [Vehicle, 0.93 ± 0.03, n = 6 cells (6 mice); AIDA, 1.26 ± 0.05, n = 6 cells (5 mice); MPEP, 1.14 ± 0.08, n = 5 cells (3 mice); $F_{2,14}$ = 10.78, P = 0.0011 Vehicle vs. AIDA, P = 0.035 Vehicle vs. MPEP, one-way ANOVA with Tukey's HSD *post hoc* test; Figure 6C]. These results indicate that whisker input-evoked mGluR5 signaling also maintains P_r in mice in the late adolescent period.

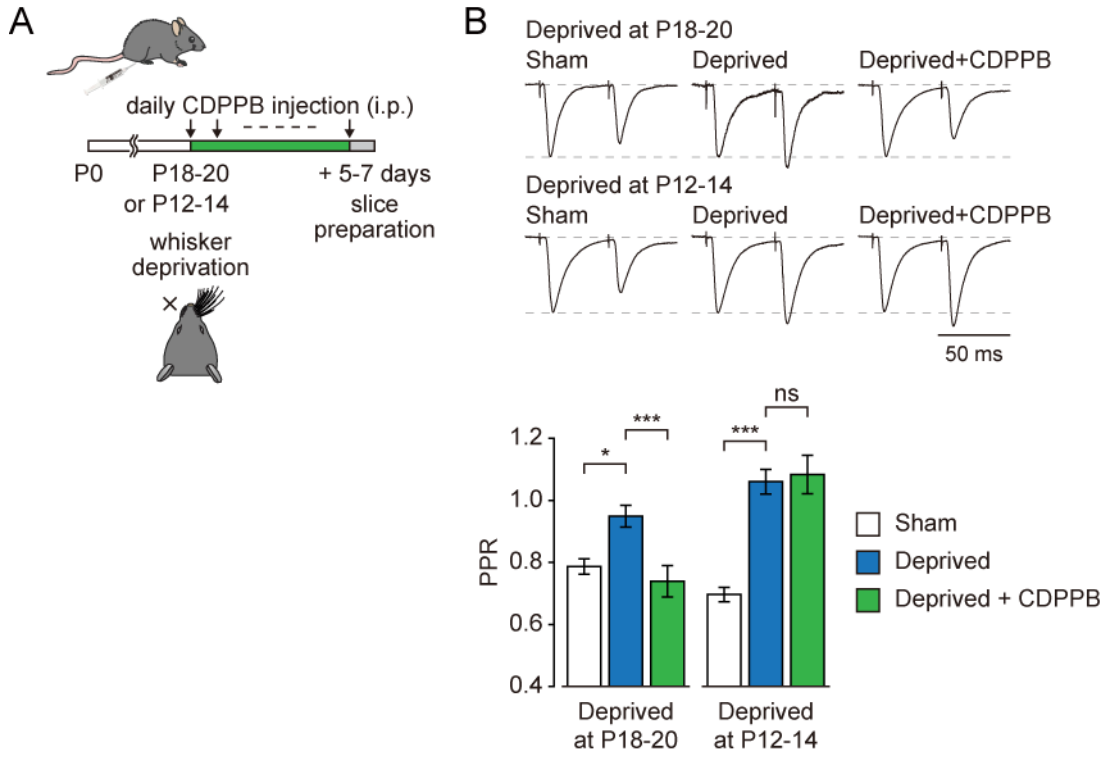

Figure 4. Pharmacological potentiation of the mGluR5 activity reverses the effects of whisker deprivation at L4–L2/3 synapses.

(A) Schema of experiment procedure. Whisker deprivation was performed at either P18–20 or P12–14 and the animals were given daily administration of CDPPB (10 mg kg^{-1}, i.p.) for 5–7 days before slice preparation.

(B) (*Upper*) Representative recordings of PPR. (*Lower*) Summary of CDPPB effects on PPR. Sham and Deprived in P18–20 or P12–14 are the same data as in Figure 1C or 3B. Mean ± SEM [n = 7 (6 mice) for Sham, n = 7 (7 mice) for Deprived, and n = 6 (4 mice) for Deprived + CDPPB in P18–20, n = 6 (5 mice) for Sham, n = 6 (6 mice) for Deprived and n = 6 (4 mice) for Deprived + CDPPB in P12–14]. ns; not significant, *P < 0.05 ***P < 0.001, one-way ANOVA with Tukey's HSD *post hoc* test.

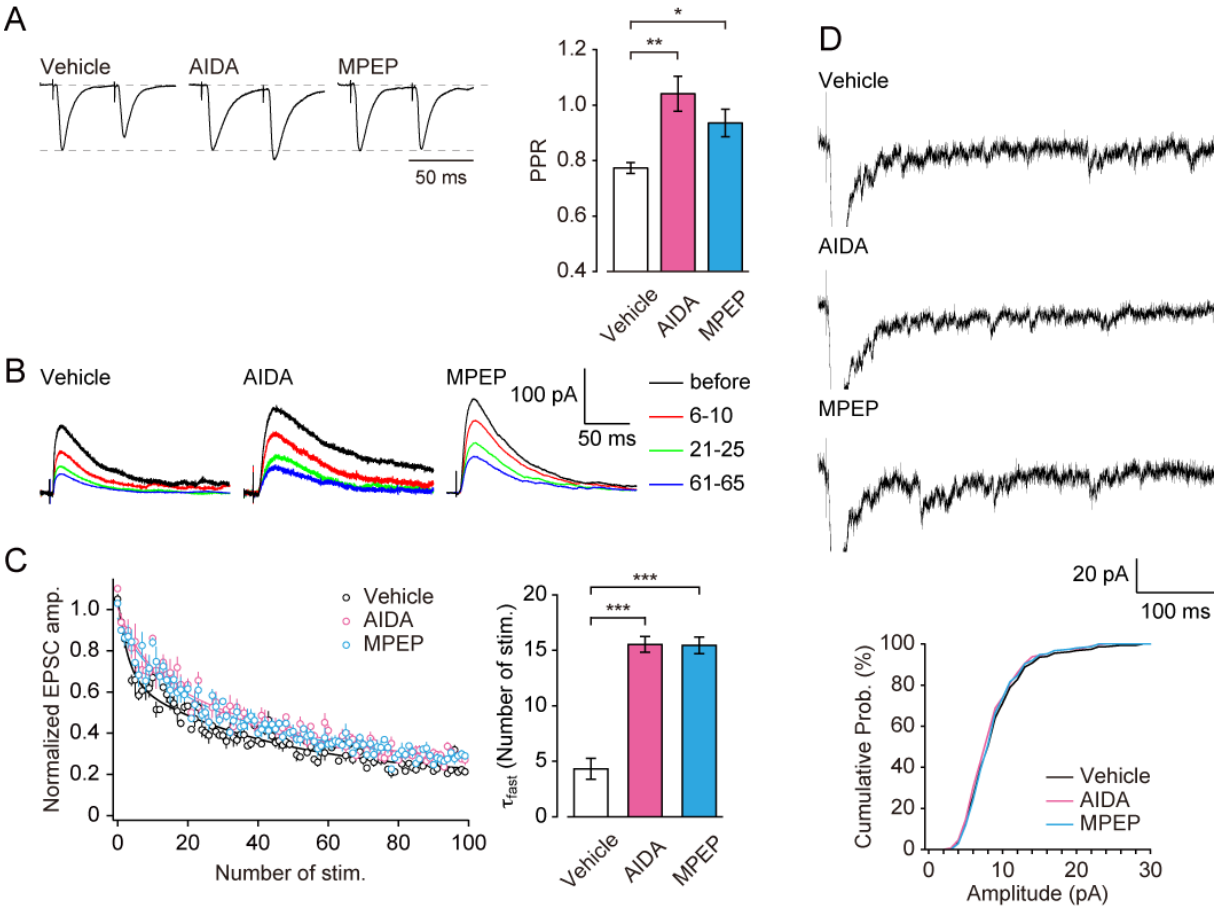

Figure 5. Pharmacological blockade of mGluR5 reproduced the effect of whisker deprivation.

(A) AIDA (1 mg kg^{-1}, i.p.) or MPEP (1 mg kg^{-1}, i.p.) was administered to whisker-intact mice (P20–22). Twenty-four hours after injection, slices were prepared. (*Left*) Representative recordings of PPR. (*Right*) Summary of drug-induced PPR changes. Mean ± SEM [n = 7 (7 mice) for Vehicle, n = 6 (6 mice) for AIDA and n = 6 (6 mice) for MPEP]. *P< 0.05, **P< 0.01, one-way ANOVA with Tukey's HSD *post hoc* test.

(B, C) Measurement of P_r using MK-801 (10 μM). (B) Representative traces of NMDAR-EPSCs. (C) (*left*) Decay time course of NMDAR-mediated EPSC in the presence of MK-801. (*right*) Summary of decay time constant. Mean ± SEM [n = 4 (4 mice) for each groups]. ***P < 0.001, one-way ANOVA with Tukey's HSD *post hoc* test.

(D) (*Upper*) Representative recordings of quantal EPSCs in ACSF containing Sr^{2+} (3 mM). (*Lower*) Cumulative histogram showing the distribution of quantal EPSC amplitude. P = 0.299 (Vehicle vs. AIDA), P = 0.999 (Vehicle vs. MPEP), Kolmogorov–Smirnov test [Vehicle; 313 events from 6 cells (6 mice), AIDA; 308 events from 6 cells (6 mice), MPEP; 311 events from 6 cells (6 mice)].

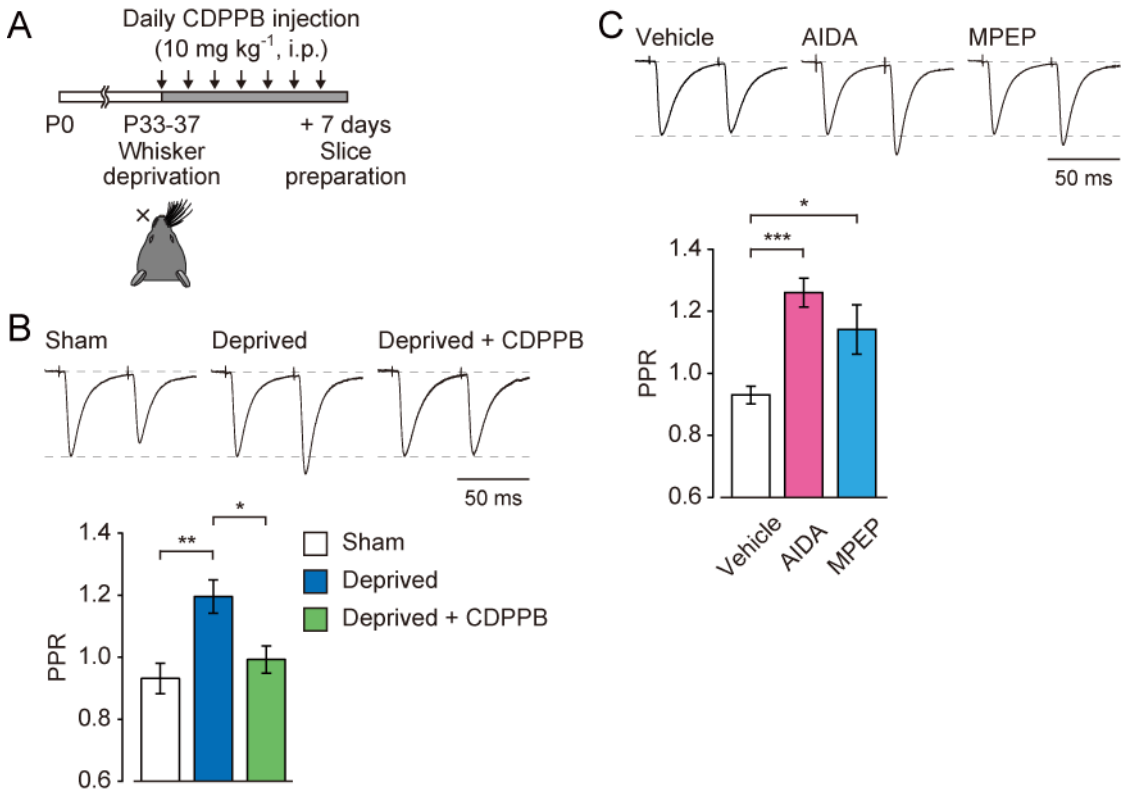

Figure 6. Whisker deprivation-induced plasticity in later stages of adolescence.

(A) Schema of experimental procedure. At P33–37, all the whiskers on the left side were plucked. Whisker deprivation was continued for 7 days before slice preparation. CDPPB (10 mg kg^{-1}, i.p.) was administered daily to whisker deprived mice.

(B) (*Upper*) Representative recordings of paired-pulse EPSC. (*Lower*) Summary of PPR. Mean ± SEM [n = 5 (5 mice) for Sham, n = 6 (5 mice) for Deprived and n = 5 (5 mice) for Deprived + CDPPB]. *P < 0.05, **P < 0.01, one-way ANOVA with Tukey's HSD *post hoc* test.

(C) Three days of daily administration of AIDA (1 mg kg^{-1}, i.p.) or MPEP (1 mg kg^{-1}, i.p.) was performed to whisker-intact mice (P39–42). (*Upper*) Representative recordings of PPR. (*Lower*) Summary of drug-induced PPR changes. Mean ± SEM [n = 6 (6 mice) for Vehicle, n = 6 (5 mice) for AIDA and n = 5 (3 mice) for MPEP]. *P < 0.05, ***P < 0.001, one-way ANOVA with Tukey's HSD *post hoc* test.

Reduction of P_r by postsynaptic neuron-specific suppression of IP_3 signaling

I next looked into the mGluR5-dependent P_r maintenance mechanism. Group I mGluRs, including mGluR5, drive G_q-related signaling in neurons throughout the cortical layers at both pre- and postsynaptic sites (Blue et al., 1997; Lopez-Bendito et al., 2002). In addition, mGluR5 activation induces Ca^{2+} responses in cortical astrocytes (Wang et al., 2006). Therefore, the site of action of the pharmacological modification of mGluR5 remains elusive. Here, I focused on the role of postsynaptic IP_3 signaling in L2/3 neurons according to the previous work in our laboratory (Furutani et al., 2006). IP_3 production in L2/3 pyramidal neurons *in vivo* was suppressed by the exogenous expression of IP_3 5-phosphatase (5ppase), which selectively hydrolyzes IP_3 (Laxminarayan et al., 1994). Our laboratory has previously demonstrated the effectiveness of 5ppase-mediated suppression of IP_3 signaling in neurons and glial cells (Furutani et al., 2006; Kanemaru et al., 2013; Kanemaru et al., 2007; Mashimo et al., 2010). To chronically express 5ppase in L2/3 pyramidal neurons, I generated an AAV vector bicistronically expressing tdTomato and $5ppase^{WT}$ under the control of a calcium/calmodulin-dependent protein kinase II alpha (CaMKIIα) promoter, favoring expression within pyramidal neurons (AAV9-CaMKIIα-tdTomato-P2A-HA-$5ppase^{WT}$; Figure 7A). I also generated an AAV vector transducing the catalytically inactive mutant (R343A/R350A) of 5ppase ($5ppase^{Inact}$) as a negative control (Communi et al., 1996;

Kanemaru et al., 2007). To validate the suppression of IP_3 signaling, I first measured mGluR-induced Ca^{2+} responses in AAV-transduced neurons in culture. The application of (*S*)-3,5-dihydroxyphenylglycine (DHPG), a group I mGluR agonist, induced Ca^{2+} responses in neurons expressing $5ppase^{Inact}$, whereas no response was observed in neurons expressing $5ppase^{WT}$ (Figure 7B). AAV vectors were injected into the barrel cortex of whisker-intact mice (P28–32) to preferentially infect L2/3 pyramidal neurons (Figure 8A). Neurons in L4 and deeper layers were sparsely infected to minimize the effect on presynaptic neurons (Figure 8A). The virus-infected L2/3 neurons showed a regular spiking pattern upon current injection, and no difference in excitability was observed between $5ppase^{WT}$- and $5ppase^{Inact}$-expressing neurons (Figure 8B). The PPR at L4–L2/3 synapses was significantly higher when recorded in postsynaptic neurons expressing $5ppase^{WT}$ than in neurons expressing $5ppase^{Inact}$ [$5ppase^{Inact}$, 0.92 ± 0.10, n = 6 cells (4 mice); $5ppase^{WT}$, 1.16 ± 0.06, n = 6 cells (5 mice); t_{10} = 3.41, P = 0.006; two-tailed unpaired Student's t-test; Figure 9A]. I confirmed that suppression of the IP_3 production had no effect on postsynaptic responsiveness by analyzing Sr^{2+}-induced asynchronous EPSCs [$5ppase^{Inact}$, 352 events from 6 cells (4 mice); $5ppase^{WT}$, 345 events from 6 cells (5 mice); P = 0.28, Kolmogorov–Smirnov test; Figure 9B]. Ongoing IP_3 signaling in postsynaptic neuron is thus necessary for the maintenance of P_r. In conclusion, these findings suggest that postsynaptic mGluR5-IP_3

signaling, which is activated in an ongoing manner by whisker inputs, is responsible for maintaining P_r at L4–L2/3 synapses in adolescent mice.

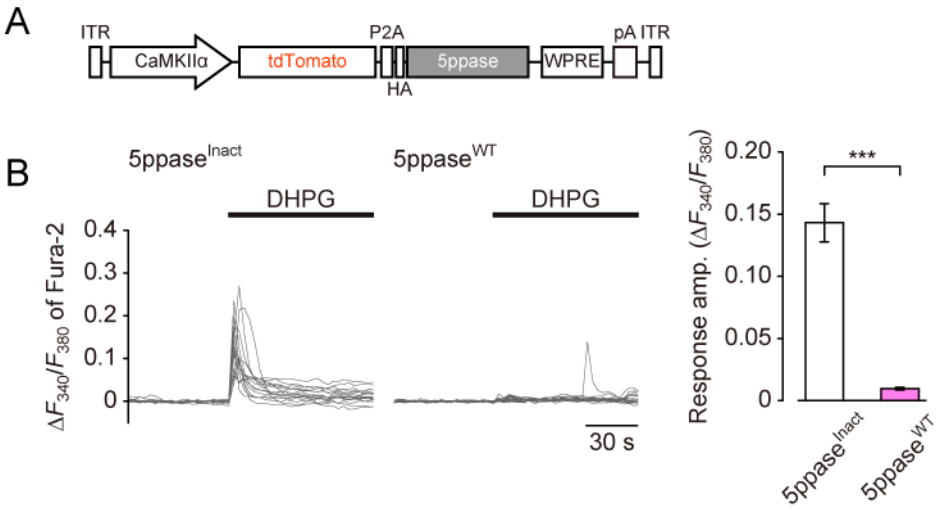

Figure 7. The suppression of mGluR-induced IP_3 production by AAV-mediated expression of 5ppase.

(A) Structure of AAV vector. ITR, inverted terminal repeats; WPRE, woodchuck hepatitis virus post-transcriptional regulatory element; pA, human growth hormone polyadenylation signal sequence.

(B) (*Left*) DHPG (50 μM)-induced Ca^{2+} responses were recorded using Fura-2 (F_{340}/F_{380}) in cultured cortical neurons expressing $5ppase^{Inact}$ (n = 16 cells) or $5ppase^{WT}$ (n = 19 cells). (*Right*) Summary of DHPG-induced Ca^{2+} response amplitudes. Mean ± SEM. ***P < 0.001, two-tailed unpaired Student's t-test.

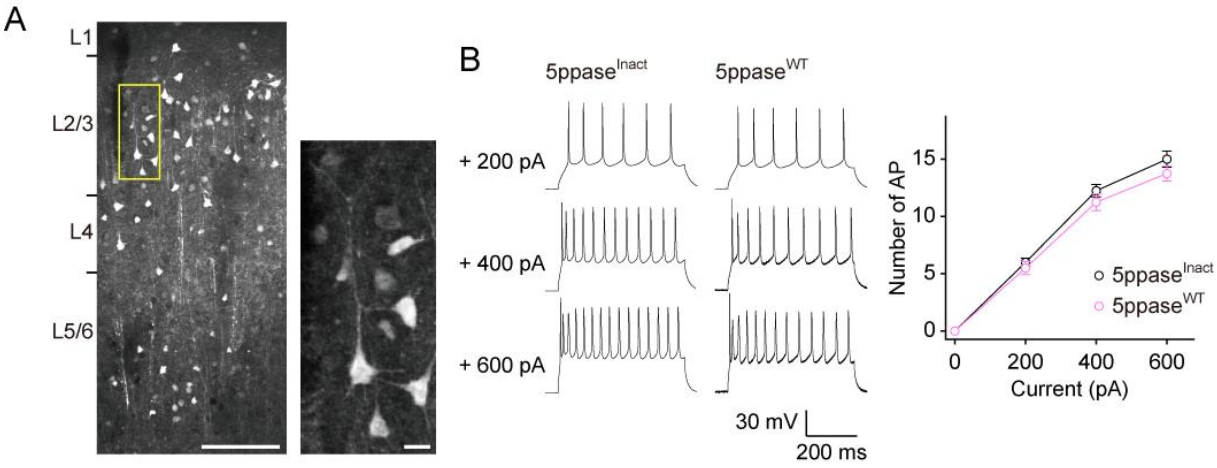

Figure 8. AAV-mediated expression of 5ppase in L2/3 pyramidal neuron.

(A) (*Left*) Representative tdTomato image of AAV-infected neurons in the barrel cortex. Scale bar, 100 µm. (*Right*) Magnification of the infected L2/3 pyramidal cells (indicated by the box in the left image). Scale bar, 10 µm.

(B) (*Left*) Representative action potential firing patterns in response to 500 ms current injections into AAV-infected L2/3 neurons. (*Right*) Summary of input current versus action potential frequency relationships shows that the excitability is same between 5ppase^{Inact}- and 5ppase^{WT}-expressing neurons. Mean ± SEM [n = 4 (2 mice) for each group].

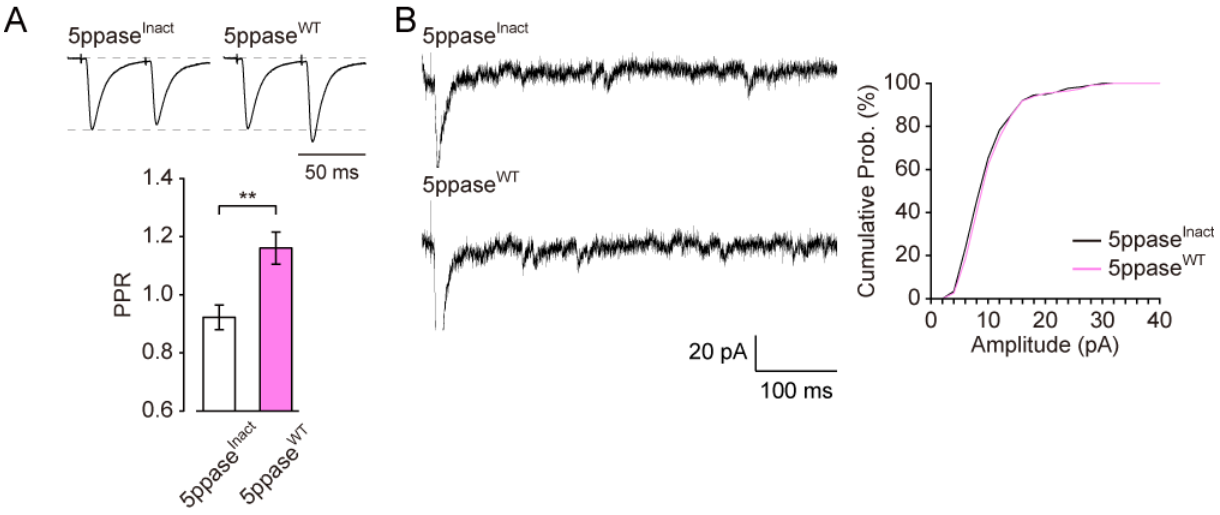

Figure 9. Reduction of P_r by postsynaptic suppression of IP_3 signaling.

(A) (*Upper*) Representative recordings of paired-pulse EPSC. (*Lower*) Summary of the effects of 5ppase on PPR. Mean ± SEM [n = 6 (4 mice) for 5ppase^{Inact} and n = 6 (5 mice) for 5ppase^{WT}]. $^{**}P < 0.01$, two-tailed unpaired Student's t-test.

(B) (*Left*) Representative recordings of quantal EPSCs in ACSF containing Sr^{2+} (3 mM). (*Right*) Cumulative histogram showing the distribution of quantal EPSC amplitude. P = 0.28, Kolmogorov–Smirnov test [5ppase^{Inact}, 352 events from 6 cells (4 mice); 5ppase^{WT}, 345 events from 6 cells (5 mice)].

Discussion

The down-regulation of neural responses resulting from deprived sensory input is a major component of cortical plasticity during development and afterwards (Feldman and Brecht, 2005). This study revealed that whisker deprivation or blockade of mGluR5-IP_3 signaling decreases P_r at L4–L2/3 synapses in adolescent mice without the alteration of postsynaptic glutamate responsiveness. This P_r reduction is a strong candidate mechanisms underlying whisker deprivation-induced depression in the barrel cortex in adolescent mice because whisker deprivation depresses responsiveness in L2/3 but not in L4 *in vivo* (Diamond et al., 1994; Glazewski and Fox, 1996; Stern et al., 2001). I propose that ongoing whisker inputs evoke mGluR5-IP_3 signaling in the postsynaptic L2/3 neurons to maintain the presynaptic function, and shutdown of this maintenance mechanism by whisker deprivation results in a reduction of P_r (Figure 10).

Postnatal development impacts experience-dependent plasticity (Hensch, 2004). In this work, I clarified a developmental shift in the molecular mechanism underlying whisker deprivation-induced depression. Up to the third postnatal week, CB1R-dependent presynaptic depression at L4–L2/3 synapses contributes to the whisker deprivation-induced depression in the barrel cortex (Li et al., 2009). Beyond this time point, the role of CB1R diminishes and,

up until at least six weeks postnatal, whisker deprivation should induce presynaptic depression at L4–L2/3 synapses due to impairment of postsynaptic mGluR5-IP_3-dependent maintenance mechanism. Several reports suggest that experience-dependent potentiation but not depression is induced in the barrel cortex in adult animals (Fox, 2002; Fox and Wong, 2005; Glazewski et al., 1996; Sawtell et al., 2003). Therefore, it is possible that mGluR5-dependent P_r maintenance mechanism is specific for adolescent animals, although this remains to be tested in adult animals. The shift from CB1R to mGluR5 modulation of synaptic plasticity may be due to the fact that rapid formation and elaboration of synapses in the rodent neocortex has subsided by the end of the third postnatal week; by then, most of the circuit structure is established (Bender et al., 2003; Micheva and Beaulieu, 1996; Shepherd et al., 2003; Stern et al., 2001). Once formed, synapses must be maintained for reliable information processing and storage, and we propose that the mGluR5-dependent P_r maintenance mechanism plays a role in synapses that are physiologically active. This mGluR5-dependent mechanism should regulate synaptic strength in combination with other mechanisms, including a PKA-dependent potentiation mechanism, in adolescent mice (Hardingham et al., 2008).

Previous studies reported that plucking a single row of whiskers in rats, beginning at P16–19, decreases P_r at L4–L2/3 synapses in a CB1R-dependent manner (Bender et al.,

2006a; Bender et al., 2006b; Li et al., 2009). Since one-row whisker deprivation is expected to result in an alteration in the input timing at the L4–L2/3 synapses between the inputs from deprived whiskers and surrounding spared whiskers, it has been proposed that spike-timing-dependent plasticity underlies the CB1R-dependent P_r depression (Bender et al., 2006b; Celikel et al., 2004; Feldman, 2000, 2012; Li et al., 2009). However, I observed CB1R-dependent P_r depression at L4–L2/3 synapses, when all whiskers were unilaterally plucked starting from P12–14 in mice. This result indicates that surrounding spared whiskers are dispensable for the CB1R-dependent P_r depression, suggesting that mechanism(s) other than spike-timing-dependent plasticity may also be involved in the plasticity.

In order for postsynaptic IP_3 signaling to regulate presynaptic function, there must be retrograde messenger(s) from the postsynapse to the presynapse. One of the known retrograde modulators of synaptic transmission, the endocannabinoid-CB1R signaling system (Regehr et al., 2009), is involved in the presynaptic depression induced by one-row whisker deprivation up to P25 in rats (Bender et al., 2006a; Bender et al., 2006b; Li et al., 2009). However, the contribution of CB1R-dependent mechanism seemed to be limited in my experimental condition (all whisker deprivation after P18 in mice). This apparent difference might be explained by the difference in the way of whisker deprivation (one-row whisker deprivation vs. all whisker deprivation), because synaptic plasticities induced by different sensory

manipulations do not necessarily share the same mechanism (Feldman and Brecht, 2005). Another candidate modulator is presynaptic mGluR-dependent signaling. Activation of group I mGluRs at presynaptic sites potentiates P_r (Perea and Araque, 2007). Therefore, ongoing elevation or reduction of this mechanism could potentially account for the present study. However, this presynaptic mGluR-dependent mechanism reportedly requires activation of CB1Rs in the surrounding astrocytes (Navarrete and Araque, 2010) and thus is inconsistent with the present results; I plan to explore the potential of glutamate as a retrograde messenger in future studies. On the other hand, our laboratory previously reported that postsynaptic mGluR1-IP_3 signaling regulates presynaptic function at the parallel fiber-Purkinje cell synapses in the cerebellar cortex and identified brain-derived neurotrophic factor (BDNF) as the retrograde messenger (Furutani et al., 2006). Furthermore, BDNF is upregulated following whisker stimulation in the mouse barrel cortex (Rocamora et al., 1996). Therefore, BDNF is a strong candidate for the retrograde messenger in the mGluR5-IP_3 dependent P_r regulation at L4–L2/3 synapses in the barrel cortex, and future studies are warranted to examine this possibility.

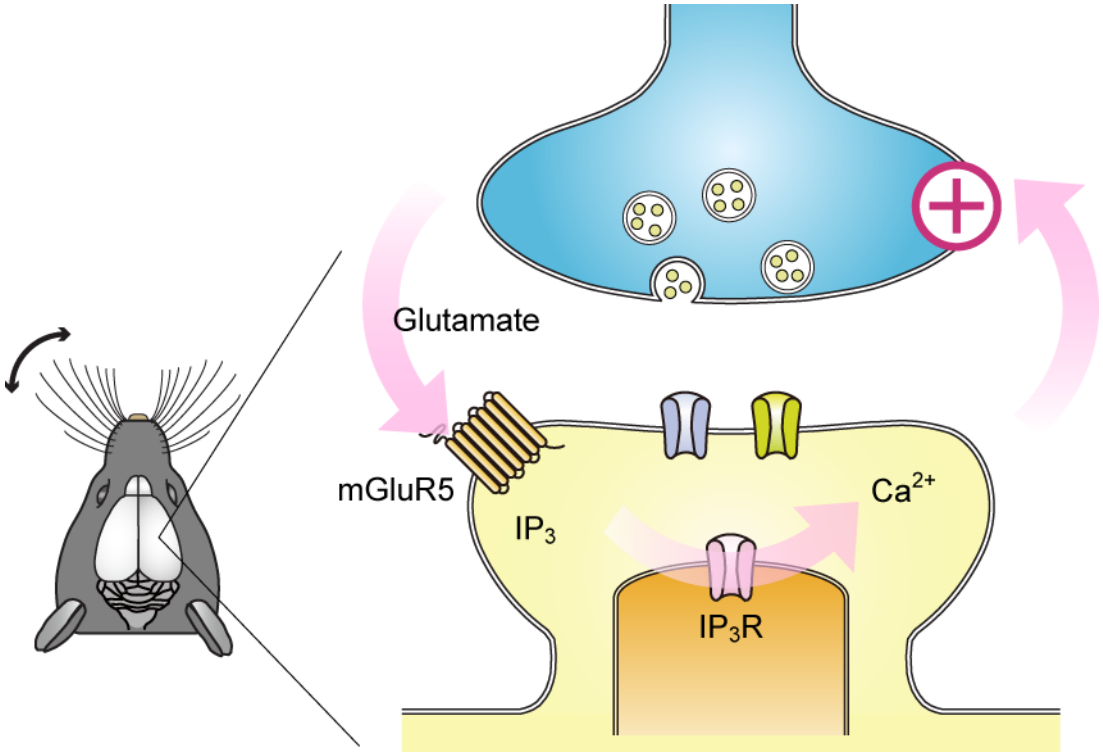

Figure 10. Proposed mechanism underlying whisker deprivation-induced depression at L4–L2/3 synapse in the barrel cortex of adolescent mice.
Postsynaptic mGluR5-IP_3 signaling, which is activated by ongoing whisker inputs, is responsible for maintaining presynaptic function in the barrel cortex of adolescent mice. Shutdown of this signaling pathway by whisker deprivation results in presynaptic depression.

References

Allen, C.B., Celikel, T., and Feldman, D.E. (2003). Long-term depression induced by sensory deprivation during cortical map plasticity in vivo. *Nat. Neurosci.* **6**, 291-299.

Armstrongjames, M., Fox, K., and Dasgupta, A. (1992). Flow of excitation within rat barrel cortex on striking a single vibrissa. *J. Neurophysiol.* **68**, 1345-1358.

Bender, K.J., Allen, C.B., Bender, V.A., and Feldman, D.E. (2006a). Synaptic basis for whisker deprivation- induced synaptic depression in rat somatosensory cortex. *J. Neurosci.* **26**, 4155-4165.

Bender, K.J., Rangel, J., and Feldman, D.E. (2003). Development of columnar topography in the excitatory layer 4 to layer 2/3 projection in rat barrel cortex. *J. Neurosci.* **23**, 8759-8770.

Bender, V.A., Bender, K.J., Brasier, D.J., and Feldman, D.E. (2006b). Two coincidence detectors for spike timing-dependent plasticity in somatosensory cortex. *J. Neurosci.* **26**, 4166-4177.

Blue, M.E., Martin, L.J., Brennan, E.M., and Johnston, M.V. (1997). Ontogeny of non-NMDA glutamate receptors in rat barrel field cortex .1. Metabotropic receptors. *J. Neurosci.* **26**, 16-28.

Buonomano, D.V., and Merzenich, M.M. (1998). Cortical plasticity: From synapses to maps. *Ann. Rev. Neurosci.* **21**, 149-186.

Celikel, T., Szostak, V.A., and Feldman, D.E. (2004). Modulation of spike timing by sensory deprivation during induction of cortical map plasticity. *Nat. Neurosci.* **7**, 534-541.

Communi, D., Lecocq, R., and Erneux, C. (1996). Arginine 343 and 350 are two active site residues involved in substrate binding by human type I D-myo-inositol 1,4,5-trisphosphate 5-phosphatase. *J. Biol. Chem.* **271**, 11676-11683.

Diamond, M.E., Huang, W., and Ebner, F.F. (1994). Laminar comparison of somatosensory cortical plasticity. *Science* **265**, 1885-1888.

Edwards, F.A., Konnerth, A., Sakmann, B., and Takahashi, T. (1989). A thin slice preparation for patch clamp recordings from neurons of the mammalian central nervous-system. *Pflug. Arch.* **414**, 600-612.

Feldman, D.E. (2000). Timing-based LTP and LTD at vertical inputs to layer II/III pyramidal cells in rat barrel cortex. *Neuron* **27**, 45-56.

Feldman, D.E. (2009). Synaptic Mechanisms for Plasticity in Neocortex. *Ann. Rev. Neurosci.* **32**, 33-55.

Feldman, D.E. (2012). The spike-timing dependence of plasticity. *Neuron* **75**, 556-571

Feldman, D.E., and Brecht, M. (2005). Map plasticity in somatosensory cortex. *Science* **310**, 810-815.

Feldmeyer, D., Lubke, J., Silver, R.A., and Sakmann, B. (2002). Synaptic connections between layer 4 spiny neurone-layer 2/3 pyramidal cell pairs in juvenile rat barrel cortex: physiology and anatomy of interlaminar signalling within a cortical column. *J. Physiol.* **538**, 803-822.

Fox, K. (2002). Anatomical pathways and molecular mechanisms for plasticity in the barrel cortex. *Neuroscience* **111**, 799-814.

Fox, K., and Wong, R.O.L. (2005). A comparison of experience-dependent plasticity in the visual and somatosensory systems. *Neuron* **48**, 465-477.

Furutani, K., Okubo, Y., Kakizawa, S., and Iino, M. (2006). Postsynaptic inositol 1,4,5-trisphosphate signaling maintains presynaptic function of parallel fiber-Purkinje cell synapses via BDNF. *Proc. Natl. Acad. Sci. USA* **103**, 8528-8533.

Glazewski, S., Chen, C.M., Silva, A., and Fox, K. (1996). Requirement for alpha-CaMKII in experience-dependent plasticity of the barrel cortex. *Science* **272**, 421-423.

Glazewski, S., and Fox, K. (1996). Time course of experience-dependent synaptic potentiation and depression in barrel cortex of adolescent rats. *J. Neurophysiol.* **75**, 1714-1729.

Glazewski, S., McKenna, M., Jacquin, M., and Fox, K. (1998). Experience-dependent depression of vibrissae responses in adolescent rat barrel cortex. *Eur. J. Neurosci.* **10**, 2107-2116.

Goda, Y., and Stevens, C.F. (1994). Two components of transmitter release at a central synapse. *Proc. Natl. Acad. Sci. USA* **91**, 12942-12946.

Hardingham, N., Wright, N., Dachtler, J., and Fox, K. (2008). Sensory deprivation unmasks a PKA-dependent synaptic plasticity mechanism that operates in parallel with CaMKII. *Neuron* **60**, 861-874.

Hensch, T.K. (2004). Critical period regulation. *Ann. Rev. Neurosci.* 27, 549-579.

Hessler, N.A., Shirke, A.M., and Malinow, R. (1993). The probability of transmitter release at a mammalian central synapse. *Nature* **366**, 569-572.

Holst, J., Szymczak-Workman, A.L., Vignali, K.M., Burton, A.R., Workman, C.J., and Vignali, D.A.A. (2006). Generation of T-cell receptor retrogenic mice. *Nat. Protoc.* **1**, 406-417.

Kakizawa, S., Yamazawa, T., Chen, Y.L., Ito, A., Murayama, T., Oyamada, H., Kurebayashi, N., Sato, O., Watanabe, M., Mori, N., *et al.* (2012). Nitric oxide-induced calcium release via ryanodine receptors regulates neuronal function. *EMBO J.* **31**, 417-428.

Kanemaru, K., Kubota, J., Sekiya, H., Hirose, K., Okubo, Y., and Iino, M. (2013). Calcium-dependent N-cadherin up-regulation mediates reactive astrogliosis and neuroprotection after brain injury. *Proc. Natl. Acad. Sci. USA* **110**, 11612-11617.

Kanemaru, K., Okubo, Y., Hirose, K., and Iino, M. (2007). Regulation of neurite growth by spontaneous Ca2+ oscillations in astrocytes. *J. Neurosci.* **27**, 8957-8966.

Kubota, J., Mikami, Y., Kanemaru, K., Sekiya, H., Okubo, Y., and Iino, M. (2016) Whisker experience-dependent mGluR signaling maintains synaptic strength in the mouse adolescent cortex. *Eur. J. Neurosci*. **44**, 2004-2014.

Laxminarayan, K.M., Chan, B.K., Tetaz, T., Bird, P.I., and Mitchell, C.A. (1994). Characterization of a cDNA-encoding the 43-kDa membrane-associated inositol-polyphosphate 5-phosphatase. *J. Biol. Chem.* **269**, 17305-17310.

Li, L., Bender, K.J., Drew, P.J., Jadhav, S.P., Sylwestrak, E., and Feldman, D.E. (2009). Endocannabinoid signaling is required for development and critical period plasticity of the whisker map in somatosensory cortex. *Neuron* **64**, 537-549.

Lopez-Bendito, G., Shigemoto, R., Fairen, A., and Lujan, R. (2002). Differential distribution of group I metabotropic glutamate receptors during rat cortical development. *Cereb. Cortex* **12**, 625-638.

Mashimo, M., Okubo, Y., Yamazawa, T., Yamasaki, M., Watanabe, M., Murayama, T., and Iino, M. (2010). Inositol 1,4,5-trisphosphate signaling maintains the activity of glutamate uptake in Bergmann glia. *Eur. J. Neurosci.* **32**, 1668-1677.

Micheva, K.D., and Beaulieu, C. (1996). Quantitative aspects of synaptogenesis in the rat barrel field cortex with special reference to GABA circuitry. *J. Comp. Neurol.* **373**, 340-354.

Min, R., and Nevian, T. (2012). Astrocyte signaling controls spike timing-dependent depression at neocortical synapses. *Nat. Neurosci.* **15**, 746-753.

Navarrete, M., and Araque, A. (2010). Endocannabinoids potentiate synaptic transmission through stimulation of astrocytes. *Neuron* **68**, 113-126.

Okubo, Y., Kakizawa, S., Hirose, K., and Iino, M. (2004). Cross talk between metabotropic and ionotropic glutamate receptor-mediated signaling in parallel fiber-induced inositol 1,4,5-trisphosphate production in cerebellar Purkinje cells. *J. Neurosci.* **24**, 9513-9520.

Okubo, Y., Sekiya, H., Namiki, S., Sakamoto, H., Iinuma, S., Yamasaki, M., Watanabe, M., Hirose, K., and Iino, M. (2010). Imaging extrasynaptic glutamate dynamics in the brain. *Proc. Natl. Acad. Sci. USA* **107**, 6526-6531.

Oliet, S.H.R., Malenka, R.C., and Nicoll, R.A. (1996). Bidirectional control of quantal size by synaptic activity in the hippocampus. *Science* **271**, 1294-1297.

Otis, T., Zhang, S., and Trussell, L.O. (1996). Direct measurement of AMPA receptor desensitization induced by glutamatergic synaptic transmission. *J. Neurosci.* **16**, 7496-7504.

Perea, G., and Araque, A. (2007). Astrocytes potentiate transmitter release at single hippocampal synapses. *Science* **317**, 1083-1086.

Regehr, W.G., Carey, M.R., and Best, A.R. (2009). Activity-dependent regulation of synapses by retrograde messengers. *Neuron* **63**, 154-170.

Rocamora, N., Welker, E., Pascual, M., and Soriano, E. (1996). Upregulation of BDNF mRNA expression in the barrel cortex of adult mice after sensory stimulation. *J. Neurosci.* **16**, 4411-4419.

Rodriguez-Moreno, A., and Paulsen, O. (2008). Spike timing-dependent long-term depression requires presynaptic NMDA receptors. *Nat. Neurosci.* **11**, 744-745.

Rosenmund, C., Clements, J.D., and Westbrook, G.L. (1993). Nonuniform probability of glutamate release at a hippocampal synapse. *Science* **262**, 754-757.

Sawtell, N.B., Frenkel, M.Y., Philpot, B.D., Nakazawa, K., Tonegawa, S., and Bear, M.F. (2003). NMDA receptor-dependent ocular dominance plasticity in adult visual cortex. *Neuron* **38**, 977-985.

Shepherd, G.M.G., Pologruto, T.A., and Svoboda, K. (2003). Circuit analysis of experience-dependent plasticity in the developing rat barrel cortex. *Neuron* **38**, 277-289.

Simons, D.J., and Land, P.W. (1987). Early experience of tactile stimulation influences organization of somatic sensory cortex. *Nature* **326**, 694-697.

Stern, E.A., Maravall, M., and Svoboda, K. (2001). Rapid development and plasticity of layer 2/3 maps in rat barrel cortex in vivo. *Neuron* **31**, 305-315.

Vanderlo.H, and Woolsey, T.A. (1973). Somatosensory cortex - structual alterations following early injury to sense organs. *Science* **179**, 395-398.

Wallace, H., and Fox, K. (1999). Local cortical interactions determine the form of cortical plasticity. *J. Neurobiol.* **41**, 58-63.

Wang, X.H., Lou, N.H., Xu, Q.W., Tian, G.F., Peng, W.G., Han, X.N., Kang, J., Takano, T., and Nedergaard, M. (2006). Astrocytic Ca^{2+} signaling evoked by sensory stimulation in vivo. *Nat. Neurosci.* **9**, 816-823.

Woolsey, T.A., and Vanderlo.H (1970). Structual organization of layer-VI in somatosensory region (SI) of mouse cerebral cortex: the description of a cortical field composed of discrete cytoarchitectonic units. *Brain Res.* **17**, 205-242.

Zhao, S.L., Ting, J.T., Atallah, H.E., Qiu, L., Tan, J., Gloss, B., Augustine, G.J., Deisseroth, K., Luo, M.M., Graybiel, A.M., *et al.* (2011). Cell type-specific channelrhodopsin-2 transgenic mice for optogenetic dissection of neural circuitry function. *Nat. Methods* **8**, 745-752.

Zucker, R.S., and Regehr, W.G. (2002). Short-term synaptic plasticity. *Ann. Rev. Neurosci.* **64**, 355-405.

Acknowledgements

First and foremost, I would like to express my gratitude to my advisor, Prof. Masamitsu Iino for constructive comments and kind encouragement throughout my graduate studies. Besides my advisor, I am grateful to Dr. Yohei Okubo for the constructive comments and continuous supports on my work. I would like to express my thanks to my laboratory colleagues for their technical supports and discussion.